JACS Au
AN OPEN ACCESS JOURNAL OF THE AMERICAN CHEMICAL SOCIETY

pubs.acs.org/jacsau

Article

Revision of the Peniroquesine Biosynthetic Pathway by Retro-Biosynthetic Theoretical Analysis: Ring Strain Controls the Unique Carbocation Rearrangement Cascade

Taro Matsuyama,[#] Ko Togashi,[#] Moe Nakano, Hajime Sato,* and Masanobu Uchiyama*

Cite This: *JACS Au* 2023, 3, 1596−1603

Read Online

ACCESS | Metrics & More | Article Recommendations | Supporting Information

ABSTRACT: Peniroquesine, a sesterterpenoid featuring a unique 5/6/5/6/5 fused pentacyclic ring system, has been known for a long time, but its biosynthetic pathway/mechanism remains elusive. Based on isotopic labeling experiments, a plausible biosynthetic pathway to peniroquesines A−C and their derivatives was recently proposed, in which the characteristic peniroquesine-type 5/6/5/6/5 pentacyclic skeleton is synthesized from geranyl−farnesyl pyrophosphate (GFPP) via a complex concerted A/B/C-ring formation, repeated reverse-Wagner−Meerwein alkyl shifts, three successive secondary (2°) carbocation intermediates, and a highly distorted *trans*-fused bicyclo[4.2.1]nonane intermediate. However, our density functional theory calculations do not support this mechanism. By applying a retro-biosynthetic theoretical analysis strategy, we were able to find a preferred pathway for peniroquesine biosynthesis, involving a multistep carbocation cascade including triple skeletal rearrangements, *trans-cis* isomerization, and 1,3-H shift. This pathway/mechanism is in good agreement with all of the reported isotope-labeling results.

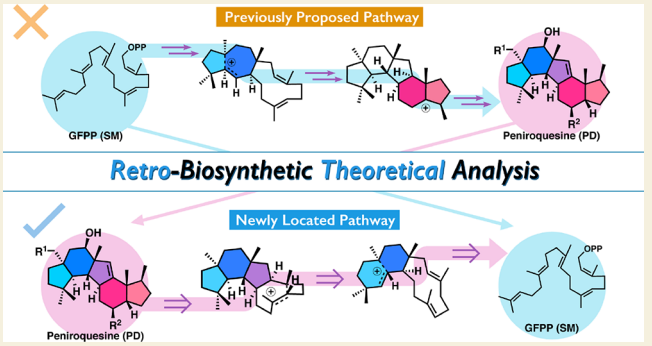

KEYWORDS: *terpene, density functional theory, retro-biosynthetic analysis, rearrangement, ring strain*

Terpenes/terpenoids have diverse chemical structures and a wide range of bioactivities. Their structural diversity arises from a series of carbocation-stitching reactions of simple unsaturated hydrocarbons, orchestrated by terpene cyclases (TCs).[1−3] Since this carbocation cascade proceeds rapidly and sequentially inside TCs, it is difficult to analyze the reaction mechanisms by means of experimental methods alone, such as the isolation of intermediates and isotope-labeling experiments. To overcome this limitation, combinations of experimental and computational chemistry have been actively pursued to elucidate complex biosynthetic mechanisms.[4−15] In this study, we describe a "retro-biosynthetic theoretical analysis" strategy[15−21] employing density functional theory (DFT). This strategy of retro-biosynthetic analysis and calculation from the product side allows us to eliminate a vast number of possibilities because the conformation of the final product is relatively fixed in contrast to the high conformational flexibility of the starting materials. In combination with previous experimental findings, this approach enabled us to delineate in detail the whole biosynthetic pathway leading to peniroquesine.

Sesterterpenes represent the least common group of terpenes but have various bioactivities, such as anticancer, antimicrobial, and anti-inflammatory activities.[22,23] Recently, Cai et al. isolated and characterized peniroquesines A−C and their derivatives, possessing a unique 5/6/5/6/5 fused pentacyclic ring system, from the fungus *Penicillium roqueforti* YJ-14.[24] They also examined the biological activities and proposed a biosynthetic pathway to peniroquesine on the basis of isotope-labeling experiments (Figure 1). However, their putative reaction mechanism includes several problematic steps. For example, the A/B/C rings are constructed by a unique skeletal rearrangement (**ii** → **iii**, Path I; Figure 1B) involving four bond recombinations in one step, but such highly concerted skeletal rearrangement would require strict conformation fixation to provide orbital overlap. On the other hand, a stepwise A/B/C-ring formation mechanism (Path II) would involve a series of three successive secondary (2°) carbocation intermediates, which are expected to be much more unstable than the tertiary (3°) carbocations.[25−27] Also, the *trans*-fused bicyclo[4.2.1]nonane intermediate (**viii**) in their proposed mechanism seems implausible because of its

Received: January 20, 2023
Revised: April 22, 2023
Accepted: April 24, 2023
Published: May 15, 2023

https://doi.org/10.1021/jacsau.3c00039
JACS Au 2023, 3, 1596−1603

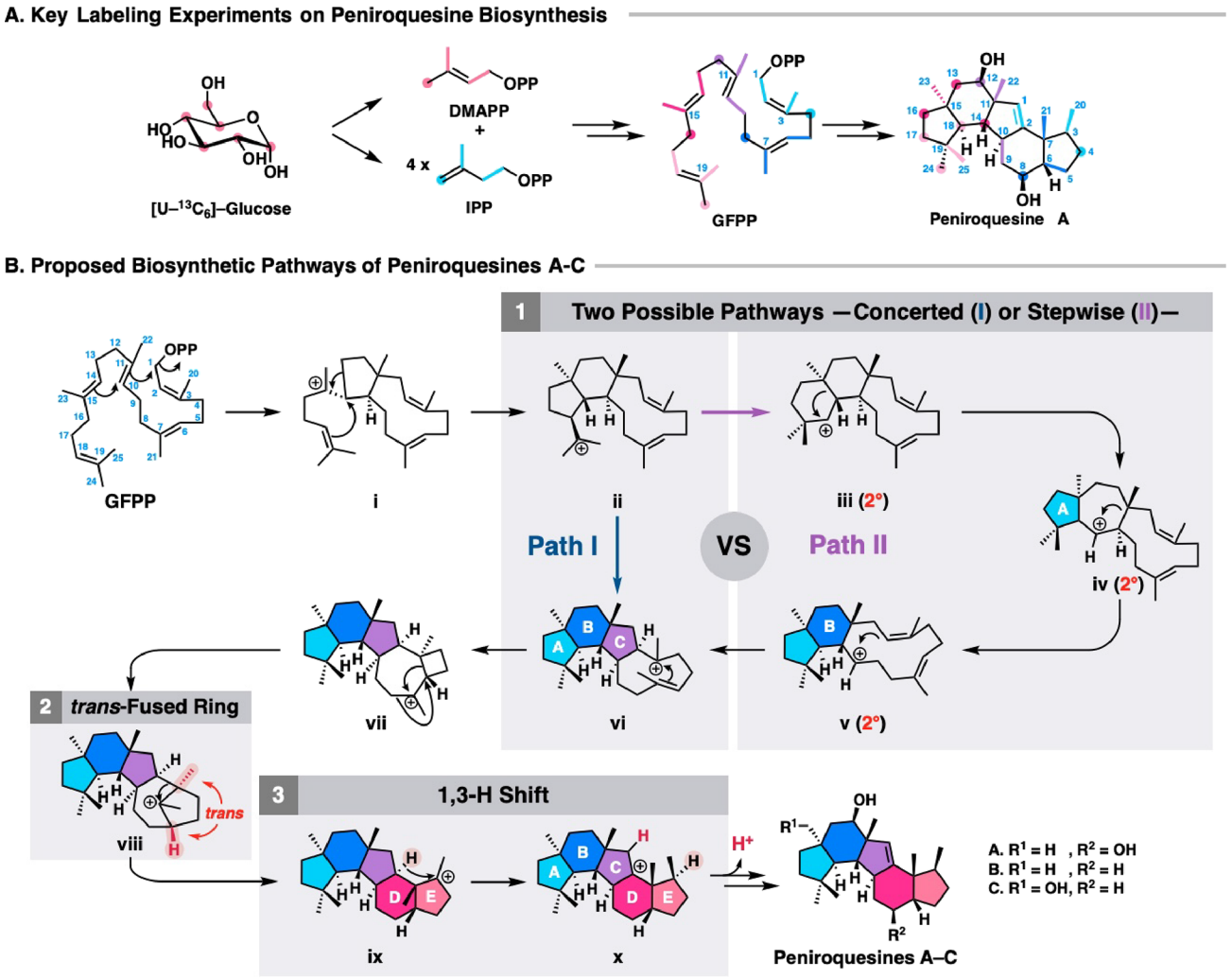

Figure 1. Previous work on peniroquesine biosynthesis. (A) Reported isotope-labeling results. (B) Proposed biosynthetic pathways.

extremely high ring strain. In addition, they proposed a 1,3-H shift across two rings (**ix** → **x**), even though 1,3-H shifts are generally rare compared to 1,2-, 1,4-, and 1,5-H shifts and require high activation energy.[6,28] Thus, further evaluation of the enigmatic biosynthetic pathway and reaction mechanisms of peniroquesine seems worthwhile. The aims of the present study are as follows: (i) to uncover the entire reaction pathway of the continuous carbocation cascade leading to the unique 5/6/5/6/5 pentacyclic skeleton of peniroquesine; (ii) to investigate the reaction mechanisms through which the complex framework and stereochemistry are produced; and in particular, (iii) to examine whether the highly concerted transannular reaction to construct the A/B/C rings (**ii** → **iii**) and the 1,3-H shift occurs in a stepwise or concerted manner.

We began our study by applying density functional theory (DFT) calculations to the proposed pathway of peniroquesine biosynthesis. We found that the results did not support the proposed pathway/mechanism. Despite methodological advances in quantum-chemical calculations, theoretical studies of complicated biosynthetic processes that involve extensive bond rearrangements remain challenging, partly because of the existence of many possible associated pathways/conformations/mechanisms. Most previous theoretical studies of complex biosynthetic reactions have examined only a few selected pathways, chosen rather arbitrarily on the basis of experimentally proposed pathway(s)/mechanism(s).[29−31] We have recently established a powerful combination of quantum-chemical calculations with the global reaction route mapping (GRRM) method[32] to unveil the complicated reaction pathways/mechanisms of biosynthetic reactions.[33−35] However, even with this method, it was extremely difficult to elucidate the biosynthesis of peniroquesine, with its characteristic pentacyclic C_{25} skeleton and eight stereogenic centers, the formation of which requires complex rearrangements or fragmentation reactions. After extensive investigations, we performed a retro-biosynthetic theoretical analysis that proved effective for this highly complicated molecule, and on the basis of these results, we propose a different route/mechanism, which is in good agreement with previous isotope-labeling experimental findings. DFT calculations combined with GRRM based on the Gaussian 16 program[36] were first employed to evaluate the peniroquesine biosynthetic pathway proposed by Cai et al. The full reaction pathway for the conversion of GFPP into **IM12** and the energy diagram (relative energies with respect to **IM1**) are shown in Scheme 1 and Figure 2 (gray dashed line), respectively. Note that transient structures leading from transition states to intermediates are included in the scheme for the sake of clarity. The dissociation of pyrophosphate from GFPP, yielding allylic carbocation **IM1**, initiates the multistep carbocation

https://doi.org/10.1021/jacsau.3c00039
JACS Au 2023, 3, 1596−1603

Scheme 1. Results of the First DFT Evaluation of the Whole Peniroquesine Biosynthetic Pathway and Potential Energy Charges in Each Structure[a]

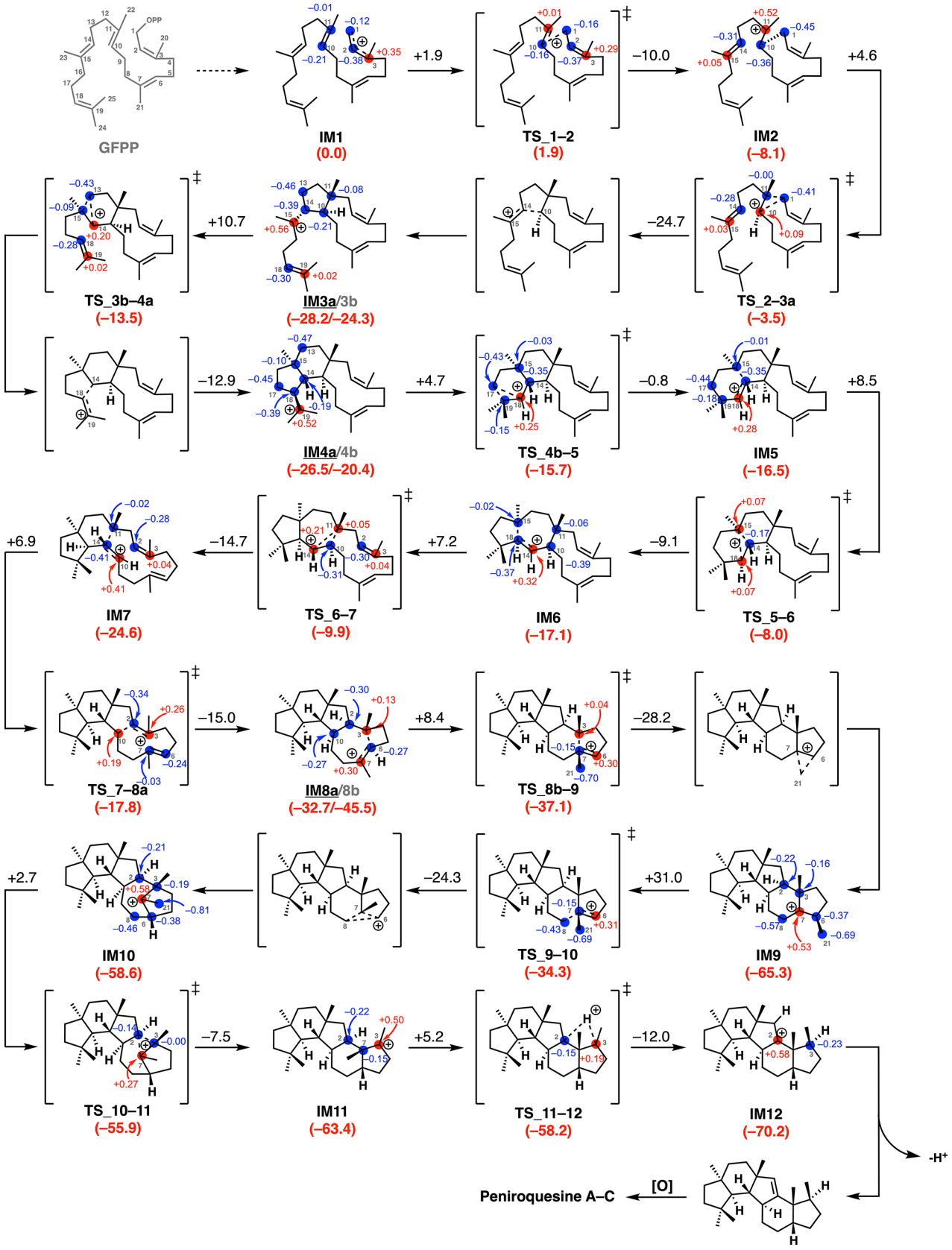

[a]Positive charge; red, negative charge; blue. Potential energies (kcal mol^{-1}, Gibbs free energies calculated at the M06-2X/6-31+G(d,p) level) relative to **IM1** are shown in parentheses.

https://doi.org/10.1021/jacsau.3c00039
JACS Au 2023, 3, 1596−1603

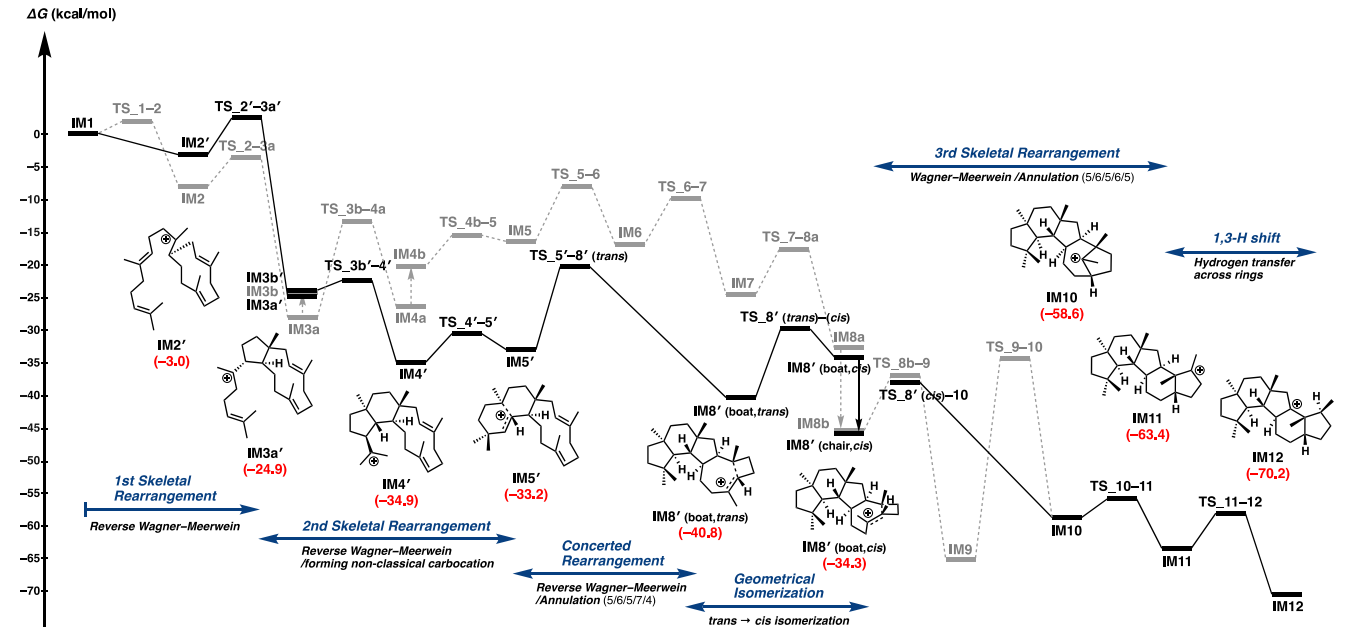

Figure 2. Energy diagram of the peniroquesine biosynthetic pathway. Potential energies (kcal mol^{-1}, Gibbs free energies calculated at the M06-2X/6-31+G(d,p) level) relative to **IM1** are shown in parentheses (gray dashed line; first calculated pathway, black solid line; recalculated pathway).

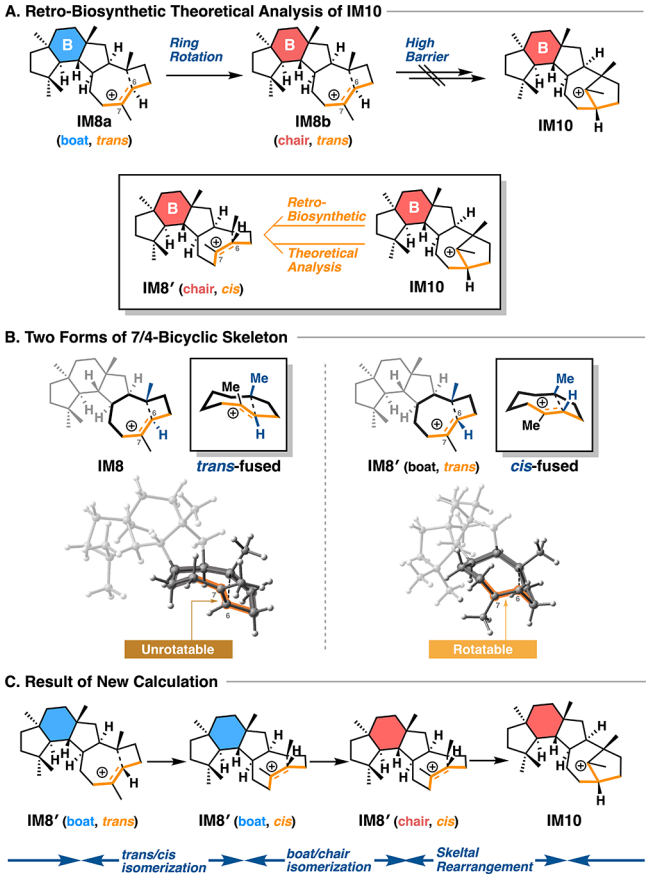

Figure 3. (A–C) Results of close analysis of the reaction from **IM8** to **IM10**.

cascade leading to peniroquesine. First, the through-space cation-π interaction between the allyl cation on **IM1** and the π-electrons on the C10–C11 double bond enables smooth annulation with a very low activation free energy of 1.9 kcal mol^{-1} to generate **IM2**, a 3° carbocation stabilized by the hyperconjugation of the C1–C10 σ-bond. Subsequently, a reverse (3° → 2°)-Wagner–Meerwein rearrangement proceeds to give the 2° carbocation, which is immediately captured by the π-electrons of the nearby C14–C15 double bond to construct the A-ring, producing a 5/11 bicyclic 3° carbocation (**IM3a**) with a large stabilization energy (−24.7 kcal mol^{-1}). After the conformational change of **IM3a** to **IM3b** with an activation barrier of 8.6 kcal mol^{-1}, the rearrangement reaction is followed by C–C σ-bond formation in a similar manner to the previous reaction (**IM2** → **IM3a**), producing a 5/6/11 tricyclic 3° carbocation (**IM4a**). Despite extensive computations, we could not find any plausible route/conformation to construct the A/B/C ring from **IM4** in a single step. Instead, we successfully located a stepwise pathway. Following the conformational change of the ^{i}Pr moiety (**IM4a** → **IM4b**), the third reverse-Wagner–Meerwein rearrangement with ring expansion takes place, producing **IM5** with a very low activation energy of 4.7 kcal mol^{-1}. The next two steps proceed in a similar manner to the 1,2-alkyl shift (**IM4b** → **IM5**), affording the intermediates **IM6** and **IM7**. These carbocation intermediates (**IM5**, **IM6**, and **IM7**) are not just 2° carbocations but appear to be non-classical carbocations in equilibrium between 3° (with a C–C double bond) and 2° (with a C–C single bond) carbocations and are therefore more stable than 2° carbocations (the relative energies of **IM5**, **IM6**, and **IM7** with respect to **IM1** are −16.5, −17.1, and −24.6 kcal mol^{-1}, respectively). **IM7** undergoes another cyclization with relatively large exothermicity (−15.0 kcal mol^{-1}) to form a 5/6/5/7/4 pentacyclic carbocation intermediate (**IM8a**) stabilized by a through-space cation-π interaction with the C6–C7 double bond. **IM8a** is then further stabilized by conformational interconversion of the B-ring (boat-form → chair-form with −12.8 kcal mol^{-1}) to yield **IM8b**. Then, annulation with a Wagner–Meerwein methyl shift proceeds to give an extremely stable and low-strain 3° carbocation **IM9** with a large stabilization energy (−28.2 kcal mol^{-1}). **IM9** undergoes reverse Wagner–Meerwein rearrangement followed by skeletal rearrangement via **TS_8b–9** to afford **IM10** possessing a *cis*-

https://doi.org/10.1021/jacsau.3c00039
JACS Au 2023, 3, 1596–1603

Scheme 2. Results of Recalculated DFT Evaluation of the Whole Peniroquesine Biosynthetic Pathway and Potential Energy Charges in Each Structure[a]

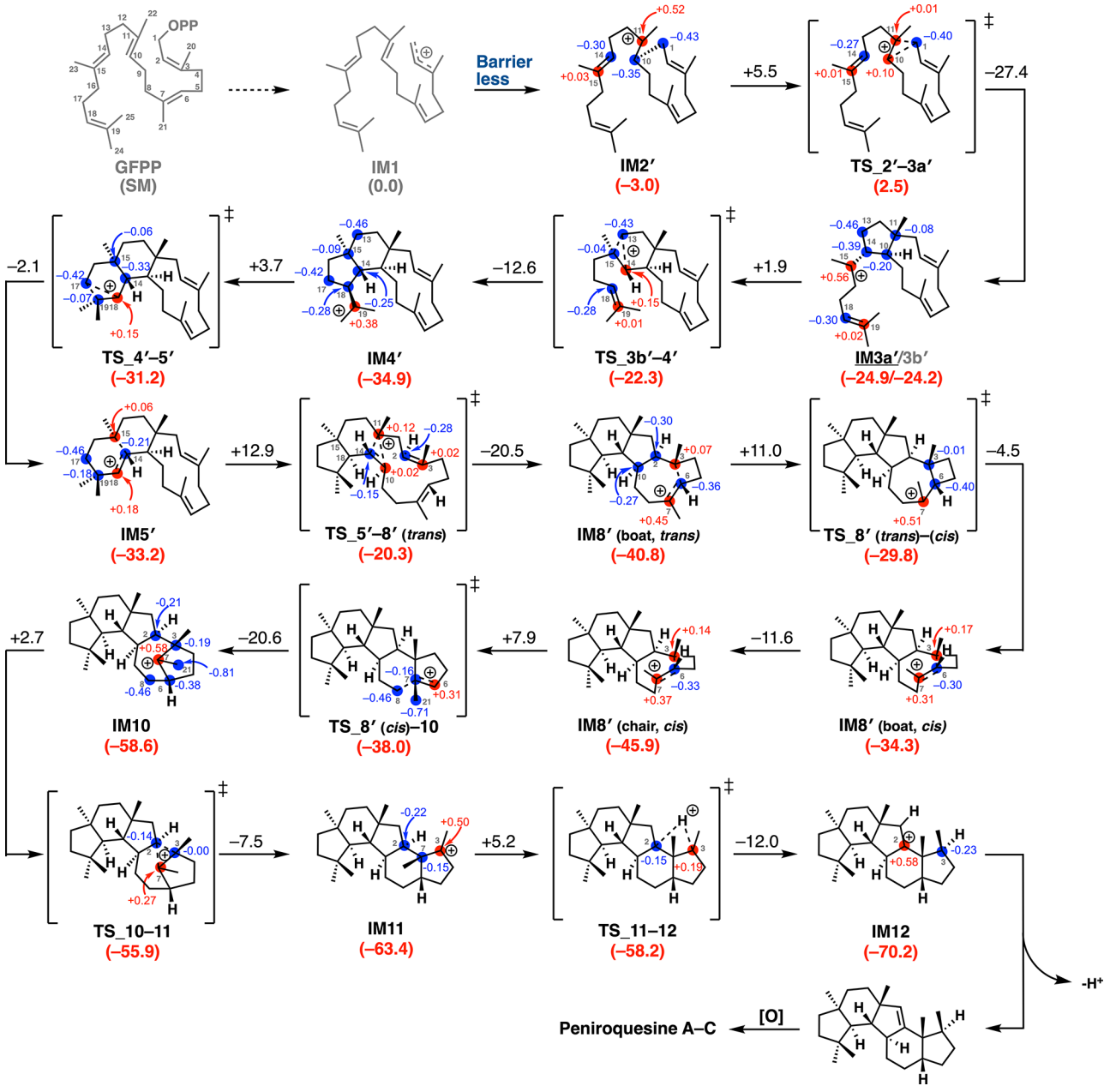

[a]Positive charge; red, negative charge; blue. Potential energies (kcal mol^{-1}, Gibbs free energies calculated at the M06-2X/6-31+G(d,p) level) relative to **IM1** are shown in parentheses.

fused bicyclo[4.2.1]nonane skeleton. Note that the *trans*-fused bicyclo[4.2.1]nonane skeleton (**E**) proposed by Cai et al. could not be optimized by DFT calculation because of its high ring strain. From **IM10**, a smooth ring-contraction reaction occurs, probably because of the distorted bicyclo structure and the good orbital overlap between the carbocation p-orbital and C2−C3 σ-bond, affording the more stable 3° carbocation, **IM11**. Interestingly, **IM11** undergoes ring-spanning 1,3-H transfer with a very small activation energy (5.2 kcal mol^{-1}) to produce **IM12**. We also investigated other possible reaction pathways from **IM11** to **IM12**, but we could not locate any other route with lower activation energies than the concerted 1,3-H shift. Finally, **IM12** is subjected to deprotonation ($-H^+$) to complete the peniroquesine skeleton.

The multistep carbocation cascade pathway described above is well aligned with the results of the isotope-feeding experiments. However, the energy diagram (Figure 2, gray dashed line) suggests that the carbocation cascade is unlikely to proceed spontaneously at ambient temperature because of the high barrier (>25 kcal mol^{-1}) to formation of the bicyclo[4.2.1]nonane skeleton (**IM9** → **TS_9–10**). Despite the high stability of **IM9** and the resulting high barrier to **TS_9–10** formation, no by-products derived from **IM9** have been identified to date. In addition, the highly energy-requiring forward and backward 1,2-methyl (C21) shift process via **IM9** seems unfavorable. However, attempts to find a reasonable pathway/mechanism to fix all of these problems were unsuccessful. Therefore, we next decided to trace the

https://doi.org/10.1021/jacsau.3c00039
JACS Au 2023, 3, 1596−1603

peniroquesine ring-construction processes in the reverse direction, starting from **IM12**, which has less flexibility of conformation. From **IM12** to **IM10**, a pathway essentially the same as that of Scheme 1 was obtained. However, careful examination of the potential energy surface (PES) around **IM10** suggested that **IM8′(chair,*cis*)** is the kinetically and thermodynamically more favorable precursor. The intermediate **IM8′(chair,*cis*)** is a geometric isomer of **IM8** with respect to the C6−C7 double bond (Figure 3A). Rotation of double bonds (*cis-trans* isomerization) requires high activation energy,[37,38] but in **IM8**, the carbocation in close proximity forms a fused 7/4 bicyclic framework in which the π-bond "partially" disappears. However, *cis-trans* isomerization of **IM8** would not occur due to the high strain caused by the *trans*-fused 7/4-bicyclic skeleton (Figure 3B). In general, TCs tightly pre-regulate the conformation of the starting materials, controlling the conformations of all reactive intermediates and the reactivity of the cationic intermediates in the active site pocket.[39−42] Hence, it seems implausible for such a large conformational change to occur in the late stage of biosynthesis. Thus, we continued the retro-biosynthetic analysis using **IM8′(chair,*cis*)** and finally located a new energetically favorable and step-economical pathway (Scheme 2 and Figure 2). After the chair-boat conformational change of the B-ring of **IM8′(chair,*cis*)** to afford **IM8′(boat,*cis*)**, bond rotation proceeds smoothly to give the *trans* isomer, **IM8′(boat,*trans*)** with the *cis*-fused 7/4-bicyclic structure (Figure 3B). Surprisingly, **IM8′(boat,*trans*)** can be generated directly from **IM5′** with a low activation energy (12.9 kcal mol^{-1}), and the two intermediates **IM6** and **IM7** are bypassed by a double-transannulation reaction. A close retro-biosynthetic computational analysis successfully located the carbocation-mediated A/B-ring formation (**IM5′** → **IM2′**), which proceeds in essentially the same manner, as shown in Scheme 1. Interestingly, **IM2′** thus obtained is generated barrierlessly from **IM1**. Key features of this new reaction pathway are as follows: (i) all of the activation barriers are sufficiently low to allow the reaction to proceed smoothly at ambient temperature; (ii) the entire energy profile descends as the reactions proceed, and the overall exothermicity is very large (ca. 70 kcal mol^{-1}); (iii) the *cis*/*trans* isomerization plays an important role in the ring construction of peniroquesine; and (iv) peniroquesine synthase fixes the initial conformation of GFPP for smooth and efficient ring construction, including complex skeletal rearrangements, 1,3-H shifts, and the *cis*/*trans* geometrical isomerization.

In conclusion, our application of the combination of computational chemistry and retro-biosynthetic analysis revealed a revised biosynthetic pathway of peniroquesine that is both more favorable than the previously proposed pathway and fully compatible with all isotope-labeling experimental findings. Because the biosynthesis of natural products is very tightly regulated in enzymes, it is extremely difficult to examine the stability and reactivity of individual putative intermediates or to determine whether a reaction is stepwise or concerted, simply on the basis of experimental studies. Thus, when calculating whole biosynthetic pathways from starting materials, it is necessary to consider a vast number of possibilities due to their high flexibility. In contrast, however, the conformation of the final product is relatively fixed, and therefore, our strategy of "retro"-biosynthetic calculations from the product side allows us to eliminate various possibilities. There are still many natural products whose biosynthetic pathways are unresolved because they involve complex skeletal rearrangement reactions and conformational transformations, and in this context, we believe that retro-biosynthetic analysis is a powerful tool to uncover these pathways. We are continuing to investigate the biosynthetic reaction pathways/mechanisms of other natural products using this approach.

METHODS

All calculations were carried out using the Gaussian 16 package.[36] Structure optimizations were done at the M06-2X level[43] in the gas phase using the 6-31+G(d,p) basis set. The vibrational frequencies were computed at the same level to check whether each optimized structure is an energy minimum (no imaginary frequency) or a transition state (single imaginary frequency). Intrinsic reaction coordinate (IRC) calculations[44−47] for all TSs were performed with GRRM17[32] to confirm the connection between the transition states and the reactants/products. The Gibbs free energy used for discussion in this study was calculated by adding the gas-phase Gibbs free energy correction.

ASSOCIATED CONTENT

Supporting Information

The Supporting Information is available free of charge at https://pubs.acs.org/doi/10.1021/jacsau.3c00039.

Computational details, 3D representation of the structure, coordinates, and energies for all computed structures (PDF)

AUTHOR INFORMATION

Corresponding Authors

Hajime Sato − *Interdisciplinary Graduate School of Medicine and Engineering, University of Yamanashi, Kofu, Yamanashi 400-8510, Japan;* orcid.org/0000-0001-5185-096X; Email: hsato@yamanashi.ac.jp

Masanobu Uchiyama − *Graduate School of Pharmaceutical Sciences, The University of Tokyo, Bunkyo-ku, Tokyo 113-0033, Japan; Research Initiative for Supra-Materials (RISM), Shinshu University, Ueda, Nagano 386-8567, Japan;* orcid.org/0000-0001-6385-5944; Email: uchiyama@mol.f.u-tokyo.ac.jp

Authors

Taro Matsuyama − *Graduate School of Pharmaceutical Sciences, The University of Tokyo, Bunkyo-ku, Tokyo 113-0033, Japan*

Ko Togashi − *Graduate School of Pharmaceutical Sciences, The University of Tokyo, Bunkyo-ku, Tokyo 113-0033, Japan*

Moe Nakano − *Interdisciplinary Graduate School of Medicine and Engineering, University of Yamanashi, Kofu, Yamanashi 400-8510, Japan*

Complete contact information is available at: https://pubs.acs.org/10.1021/jacsau.3c00039

Author Contributions

#T.M. and K.T. contributed equally to this work.

Notes

The authors declare no competing financial interest.

ACKNOWLEDGMENTS

This work was partly supported by JSPS Grant-in-Aid for Scientific Research on JSPS KAKENHI (S) (no. 17H06173),

KAKENHI (A) (no. 22H00320), Transformative Research Areas (A) (no. 22H05125), and JST CREST (no. JPMJCR19R2) as well as grants from NAGASE Science Technology Foundation, Naito Foundation, Chugai Foundation, and Uehara Memorial Foundation (to M.U.). This work was partly supported by JSPS KAKENHI Grant-in-Aid for Early-Career Scientists (no. 22K14791), an MEXT grant for Leading Initiative for Excellent Young Researchers (no. JPMXS0320200422), JST PRESTO (no. JPMJPR21D5), the Uehara Memorial Foundation (no. 202110117), the Terumo Life Science Foundation (no. 21-III4030), and a Research Grant for Young Scholars funded by Yamanashi Prefecture (to H.S.).

REFERENCES

(1) Rudolf, J. D.; Alsup, T. A.; Xu, B.; Li, Z. Bacterial terpenome. *Nat. Prod. Rep.* **2021**, *38*, 905−980.
(2) Christianson, D. W. Structural and Chemical Biology of Terpenoid Cyclases. *Chem. Rev.* **2017**, *117*, 11570−11648.
(3) Dickschat, J. S. Bacterial Terpene Cyclases. *Nat. Prod. Rep.* **2016**, *33*, 87−110.
(4) Sato, H.; Saito, K.; Yamazaki, M. Acceleration of Mechanistic Investigation of Plant Secondary Metabolism Based on Computational Chemistry. *Front. Plant. Sci.* **2019**, *10*, 802.
(5) Wei, X.; Matsuyama, T.; Sato, H.; Yan, D.; Chan, P. M.; Miyamoto, K.; Uchiyama, M.; Matsuda, Y. Molecular and Computational Bases for Spirofuranone Formation in Setosusin Biosynthesis. *J. Am. Chem. Soc.* **2021**, *143*, 17708−17715.
(6) Xu, H.; Goldfuss, B.; Dickschat, J. S. 1,2- or 1,3-Hydride Shifts: What Controls Guaiane Biosynthesis? *Chem. − Eur. J.* **2021**, *27*, 9758−9762.
(7) Lauterbach, L.; Goldfuss, B.; Dickschat, J. S. Two Diterpene Synthases from Chryseobacterium: Chryseodiene Synthase and Wanjudiene Synthase. *Angew. Chem., Int. Ed.* **2020**, *59*, 11943−11947.
(8) Jiang, Y.; Ozaki, T.; Harada, M.; Miyasaka, T.; Sato, H.; Miyamoto, K.; Kanazawa, J.; Liu, C.; Maruyama, J.; Adachi, M.; Nakazaki, A.; Nishikawa, T.; Uchiyama, M.; Minami, A.; Oikawa, H. Biosynthesis of Indole Diterpene Lolitrems: Radical-Induced Cyclization of an Epoxyalcohol Affording a Characteristic Lolitremane Skeleton. *Angew. Chem., Int. Ed.* **2020**, *59*, 17996−18002.
(9) Fujii, I.; Hashimoto, M.; Konishi, K.; Unezawa, A.; Sakuraba, H.; Suzuki, K.; Tsushima, H.; Iwasaki, M.; Yoshida, S.; Kudo, A.; Fujita, R.; Hichiwa, A.; Saito, K.; Asano, T.; Ishikawa, J.; Wakana, D.; Goda, Y.; Watanabe, A.; Watanabe, M.; Masumoto, Y.; Kanazawa, J.; Sato, H.; Uchiyama, M. Shimalactone Biosynthesis Involves Spontaneous Double Bicyclo-Ring Formation with 8π-6π Electrocyclization. *Angew. Chem., Int. Ed.* **2020**, *59*, 8464−8470.
(10) Sato, H.; Narita, K.; Minami, A.; Yamazaki, M.; Wang, C.; Suemune, H.; Nagano, S.; Tomita, T.; Oikawa, H.; Uchiyama, M. Theoretical Study of Sesterfisherol Biosynthesis: Computational Prediction of Key Amino Acid Residue in Terpene Synthase. *Sci. Rep.* **2018**, *8*, 2473.
(11) Sato, H.; Teramoto, K.; Masumoto, Y.; Tezuka, N.; Sakai, K.; Ueda, S.; Totsuka, Y.; Shinada, T.; Nishiyama, M.; Wang, C.; Kuzuyama, T.; Uchiyama, M. "Cation-Stitching Cascade:" Exquisite Control of Terpene Cyclization in Cyclooctatin Biosynthesis. *Sci. Rep.* **2016**, *5*, 18471.
(12) Weitman, M.; Major, D. T. Challenges Posed to Bornyl Diphosphate Synthase: Diverging Reaction Mechanisms in Monoterpenes. *J. Am. Chem. Soc.* **2010**, *132*, 6349−6360.
(13) Major, D. T.; Weitman, M. Electrostatically Guided Dynamics-The Root of Fidelity in a Promiscuous Terpene Synthase? *J. Am. Chem. Soc.* **2012**, *134*, 19454−19462.
(14) Rajamani, R.; Gao, J. Balancing Kinetic and Thermodynamic Control: The Mechanism of Carbocation Cyclization by Squalene Cyclase. *J. Am. Chem. Soc.* **2003**, *125*, 12768−12781.
(15) Raz, K.; Levi, S.; Gupta, P. K.; Major, D. T. Enzymatic Control of Product Distribution in Terpene Synthases: Insights from Multiscale Simulations. *Curr. Opin. Biotechnol.* **2020**, *65*, 248−258.
(16) Das, S.; Shimshi, M.; Raz, K.; Eliaz, N. N.; Mhashal, A. R.; Ansbacher, T.; Major, D. T. EnzyDock: Protein−Ligand Docking of Multiple Reactive States along a Reaction Coordinate in Enzymes. *J. Chem. Theory Comput.* **2019**, *15*, 5116−5134.
(17) Ansbacher, T.; Freud, Y.; Major, D. T. Slow-Starter Enzymes: Role of Active-Site Architecture in the Catalytic Control of the Biosynthesis of Taxadiene by Taxadiene Synthase. *Biochemistry* **2018**, *57*, 3773−3779.
(18) Dixit, M.; Weitman, M.; Gao, J.; Major, D. T. Substrate Folding Modes in Trichodiene Synthase: A Determinant of Chemo- and Stereoselectivity. *ACS Catal.* **2018**, *8*, 1371−1375.
(19) Dixit, M.; Weitman, M.; Gao, J.; Major, D. T. Chemical Control in the Battle against Fidelity in Promiscuous Natural Product Biosynthesis: The Case of Trichodiene Synthase. *ACS Catal.* **2017**, *7*, 812−818.
(20) Wang, Y.-H.; Xie, H.; Zhou, J.; Zhang, F.; Wu, R. Substrate Folding Modes in Trichodiene Synthase: A Determinant of Chemo- and Stereoselectivity. *ACS Catal.* **2017**, *7*, 5841−5846.
(21) Smith, K. M.; Lai, J. J. Syntheses of Heme D Models. *J. Am. Chem. Soc.* **1984**, *106*, 5746−5748.
(22) Hog, D. T.; Webster, R.; Trauner, D. Synthetic Approaches toward Sesterterpenoids. *Nat. Prod. Rep.* **2012**, *29*, 752−779.
(23) Liu, Y.; Wang, L.; Jung, J. H.; Zhang, S. Sesterterpenoids. *Nat. Prod. Rep.* **2007**, *24*, 1401−1429.
(24) Wang, J.-P.; Yu, J.; Shu, Y.; Shi, Y.-X.; Luo, P.; Cai, L.; Ding, Z.-T. Peniroquesines A−C: Sesterterpenoids Possessing a 5−6−5−6−5-Fused Pentacyclic Ring System from *Penicillium Roqueforti* YJ-14. *Org. Lett.* **2018**, *20*, 5853−5856.
(25) Sato, H.; Li, B.-X.; Takagi, T.; Wang, C.; Miyamoto, K.; Uchiyama, M. DFT Study on the Biosynthesis of Verrucosane Diterpenoids and Mangicol Sesterterpenoids: Involvement of Secondary-Carbocation-Free Reaction Cascades. *JACS. Au.* **2021**, *1*, 1231−1239.
(26) McCulley, C. H.; Tantillo, D. J. Secondary Carbocations in the Biosynthesis of Pupukeanane Sesquiterpenes. *J. Phys. Chem. A* **2018**, *122*, 8058−8061.
(27) Hong, Y. J.; Tantillo, D. J. How Many Secondary Carbocations Are Involved in the Biosynthesis of Avermitilol? *Org. Lett.* **2011**, *13*, 1294−1297.
(28) Sorensen, T. S. In *Stable Carbocation Chemistry*; Prakash, G. K. S.; Olah, G. A. Eds., Wiley: New York, 1996, *Chapter 3*.
(29) So far, pathways have been exhaustively located and verified in only a few cases.[29−31] Isegawa, M.; Maeda, S.; Tantillo, D. J.; Morokuma, K. Predicting Pathways for Terpene Formation from First Principles − Routes to Known and New Sesquiterpenes. *Chem. Sci.* **2014**, *5*, 1555−1560.
(30) Hong, Y. J.; Tantillo, D. J. Branching Out from the Bisabolyl Cation. Unifying Mechanistic Pathways to Barbatene, Bazzanene, Chamigrene, Chamipinene, Cumacrene, Cuprenene, Dunniene, Isobazzanene, Iso-γ-Bisabolene, Isochamigrene, Laurene, Microbiotene, Sesquithujene, Sesquisabinene, Thujopsene, Trichodiene, and Widdradiene Sesquiterpenes. *J. Am. Chem. Soc.* **2014**, *136*, 2450−2463.
(31) Zu, L.; Xu, M.; Lodewyk, M. W.; Cane, D. E.; Peters, R. J.; Tantillo, D. J. Effect of Isotopically Sensitive Branching on Product Distribution for Pentalenene Synthase: Support for a Mechanism Predicted by Quantum Chemistry. *J. Am. Chem. Soc.* **2012**, *134*, 11369−11371.
(32) Maeda, S.; Ohno, K.; Morokuma, K. Systematic Exploration of the Mechanism of Chemical Reactions: the Global Reaction Route Mapping (GRRM) Strategy Using the ADDF and AFIR methods. *Phys. Chem. Chem. Phys.* **2013**, *15*, 3683−3701.
(33) Sato, H.; Hashishin, T.; Kanazawa, J.; Miyamoto, K.; Uchiyama, M. DFT Study of a Missing Piece in Brasilane-Type Structure Biosynthesis: An Unusual Skeletal Rearrangement. *J. Am. Chem. Soc.* **2020**, *142*, 19830−19834.

https://doi.org/10.1021/jacsau.3c00039
JACS Au 2023, 3, 1596−1603

(34) Nakashima, Y.; Mitsuhashi, T.; Matsuda, Y.; Senda, M.; Sato, H.; Yamazaki, M.; Uchiyama, M.; Senda, T.; Abe, I. Structural and Computational Bases for Dramatic Skeletal Rearrangement in Anditomin Biosynthesis. *J. Am. Chem. Soc.* **2018**, *140*, 9743−9750.
(35) Sato, H.; Takagi, T.; Miyamoto, K.; Uchiyama, M. Theoretical Study on the Mechanism of Spirocyclization in Spiroviolene Biosynthesis. *Chem. Pharm. Bull.* **2021**, *69*, 1034−1038.
(36) Frisch, M. J. et al. *Gaussian 16 Revision C.01*, Gaussian, Inc.: Wallingford CT, 2016. Full citations are given in Supporting Information.
(37) Barrows, S. E.; Eberlein, T. H. Understanding Rotation about a C=C Double Bond. *J. Chem. Educ.* **2005**, *82*, 1329−1333.
(38) Douglas, J. E.; Rabinovitch, B. S.; Looney, F. S. Kinetics of the Thermal *Cis-Trans* Isomerization of Dideuteroethylene. *J. Chem. Phys.* **1955**, *23*, 315−323.
(39) Sato, H.; Mitsuhashi, T.; Yamazaki, M.; Abe, I.; Uchiyama, M. Computational Studies on Biosynthetic Carbocation Rearrangements Leading to Quiannulatene: Initial Conformation Regulates Biosynthetic Route, Stereochemistry, and Skeleton Type. *Angew. Chem., Int. Ed.* **2018**, *57*, 14752−14757.
(40) Sakamoto, K.; Sato, H.; Uchiyama, M. DFT Study on the Biosynthesis of Asperterpenol and Preasperterpenoid Sesterterpenoids: Exclusion of Secondary Carbocation Intermediates and Origin of Structural Diversification. *J. Org. Chem.* **2022**, *87*, 6432−6437.
(41) Hong, Y. J.; Tantillo, D. J. The Taxadiene-Forming Carbocation Cascade. *J. Am. Chem. Soc.* **2011**, *133*, 18249−18256.
(42) Pemberton, R. P.; Ho, K. C.; Tantillo, D. J. Modulation of Inherent Dynamical Tendencies of the Bisabolyl Cation via Preorganization in epi-isozizaene synthase. *Chem. Sci.* **2015**, *6*, 2347−2353.
(43) Zhao, Y.; Truhlar, D. G. The M06 Suite of Density Functionals for Main Group Thermochemistry, Thermochemical Kinetics, Noncovalent Interactions, Excited States, and Transition Elements: Two New Functionals and Systematic Testing of Four M06-class Functionals and 12 Other Functionals. *Theor. Chem. Acc.* **2008**, *120*, 215−241.
(44) Fukui, K. The Path of Chemical Reactions - the IRC Approach. *Acc. Chem. Res.* **1981**, *14*, 363−368.
(45) Page, M.; Doubleday, C., Jr.; McIver, J.W., Jr Following Steepest Descent Reaction Paths. The Use of Higher Energy Derivatives with *ab initio* Electronic Structure Methods. *J. Chem. Phys.* **1990**, *93*, 5634−5642.
(46) Ishida, K.; Morokuma, K.; Komornicki, A. The Intrinsic Reaction Coordinate. An *ab initio* Calculation for HNC→HCN and $H^-+CH_4 \rightarrow CH_4+H^-$. *J. Chem. Phys.* **1977**, *66*, 2153−2156.
(47) Gonzalez, C.; Schlegel, H. B. Reaction Path Following in Mass-weighted Internal Coordinates. *J. Phys. Chem.* **1990**, *94*, 5523−5527.

https://doi.org/10.1021/jacsau.3c00039
JACS Au 2023, 3, 1596−1603